Journal of Experimental Nanoscience

ISSN: 1745-8080 (Print) 1745-8099 (Online) Journal homepage: https://www.tandfonline.com/loi/tjen20

Green synthesis of zinc oxide nanoparticles using tomato *(Lycopersicon esculentum)* extract and its photovoltaic application

Prasanta Sutradhar & Mitali Saha

To cite this article: Prasanta Sutradhar & Mitali Saha (2016) Green synthesis of zinc oxide nanoparticles using tomato *(Lycopersicon esculentum)* extract and its photovoltaic application, Journal of Experimental Nanoscience, 11:5, 314-327, DOI: 10.1080/17458080.2015.1059504

To link to this article: https://doi.org/10.1080/17458080.2015.1059504

Published online: 06 Jul 2015.

Journal of Experimental Nanoscience, 2016
Vol. 11, No. 5, 314–327, http://dx.doi.org/10.1080/17458080.2015.1059504

Green synthesis of zinc oxide nanoparticles using tomato *(Lycopersicon esculentum)* extract and its photovoltaic application

Prasanta Sutradhar and Mitali Saha*

Department of Chemistry, National Institute of Technology, Agartala-799046, Tripura, India

(*Received 19 January 2015; final version received 25 May 2015*)

With an increasing awareness of green and clean energy, zinc oxide-based solar cells were found to be suitable candidates for cost-effective and environmentally friendly energy conversion devices. In this paper, we have reported the green synthesis of zinc oxide nanoparticles (ZnONPs) by thermal method and under microwave irradiation using the aqueous extract of tomatoes as non-toxic and ecofriendly reducing material. The synthesised ZnONPs were characterised by UV–visible spectroscopy (UV–vis), infra-red spectroscopy, particle size analyser, scanning electron microscopy (SEM), atomic force microscopy (AFM) and X-ray diffraction study (XRD). A series of ZnO nanocomposites with titanium dioxide nanoparticles (TiO_2) and graphene oxide (GO) were prepared for photovoltaic application. Structural and morphological studies of these nanocomposites were carried out using UV–vis, SEM, XRD and AFM. The current–voltage measurements of the nanocomposites demonstrated enhanced power conversion efficiency of 6.18% in case of ZnO/GO/ TiO_2 nanocomposite.

Keywords: amorphous materials; composites; tomato; atomic force microscopy (AFM); X-ray diffraction(XRD)

1. Introduction

Zinc oxide (ZnO) nanostructures are the forefront of research due to their unique properties and wide applications. It has many technological applications, because of its exceptional optical and electrical properties, such as thin-film transistors, gas sensors, transparent conductors, biomedical and piezoelectric applications.[1–4] ZnO is being extensively used in the fabrication of solar cells, such as quantum dot sensitised solar cells.[5,6] It is well known that ZnO is one of the most important semiconductor materials with direct wide band gap (3·2–3.37 eV) and good transparency [7] at room temperature. Besides, due to large exciton binding energy of 60 meV, it has potential applications in optoelectronic devices, such as solar cells.[8] It is expected to be an alternating material for TiO_2 because of its environment friendliness, stability and that; it can be synthesised into different shapes and sizes very easily.[9] Thin films of ZnO can be prepared by various techniques like sputtering,[10] chemical vapour deposition,[11] etc.

Recently, there is a growing necessity to develop environmentally friendly methods, which does not use toxic materials in the synthesis procedures. Till now, a large number of physical, chemical and biological methods are available to synthesise different types of

*Corresponding author. Email: mitalichem71@gmail.com

nanoparticles.[12–14] Synthesis of nanoparticles using different parts of the plants is quite novel, leading to truly green chemistry, avoiding the need of high pressure, energy, temperature and toxic chemicals and moreover, it is effective at a very affordable cost.[15–23] Recently, some of the researchers have described that the use of ecofriendly benign materials like leaf extract (aloe barbadensis),[24] bacteria [25] and fungus [26] for the synthesis of ZnO nanoparticles offers numerous advantages of eco-friendliness and compatibility for pharmaceutical and other biomedical applications.

In this work, we have systematically studied the synthesis of ZnONPs in mass level, using tomato extract by both thermal method and under microwave irradiation using different power. Thin films of nanocomposite of ZnONPs with graphene oxide (GO) and titanium dioxide nanoparticles (TiO_2) were prepared and the current–voltage measurements of these nanocomposites were studied for their suitable application in solar cells.

2. Materials and methods

Tomatoes were purchased from the local market of Tripura. GO was synthesised from graphite powder using modified Hummer's method.[27] Zinc nitrate and TiO_2 were purchased from Sigma Aldrich. Double distilled water was used throughout the experiments.

2.1. Preparation of tomato extract

The red tomatoes (*Lycopersicon esculentum*) was collected from the local market and washed with double distilled water. The skin was removed from the tomato and the whole mass was squeezed to get the juice. This juice was dissolved in distilled water and filtered using a Whatman filter paper (Maidstone, UK). A flow chart is given below

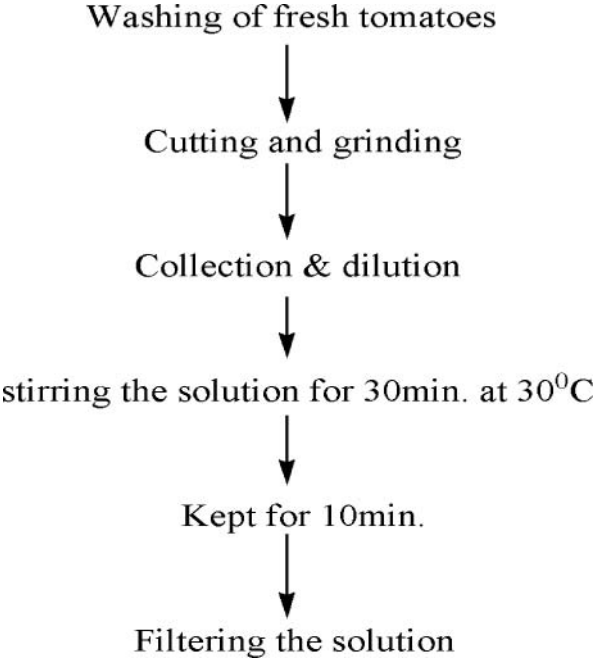

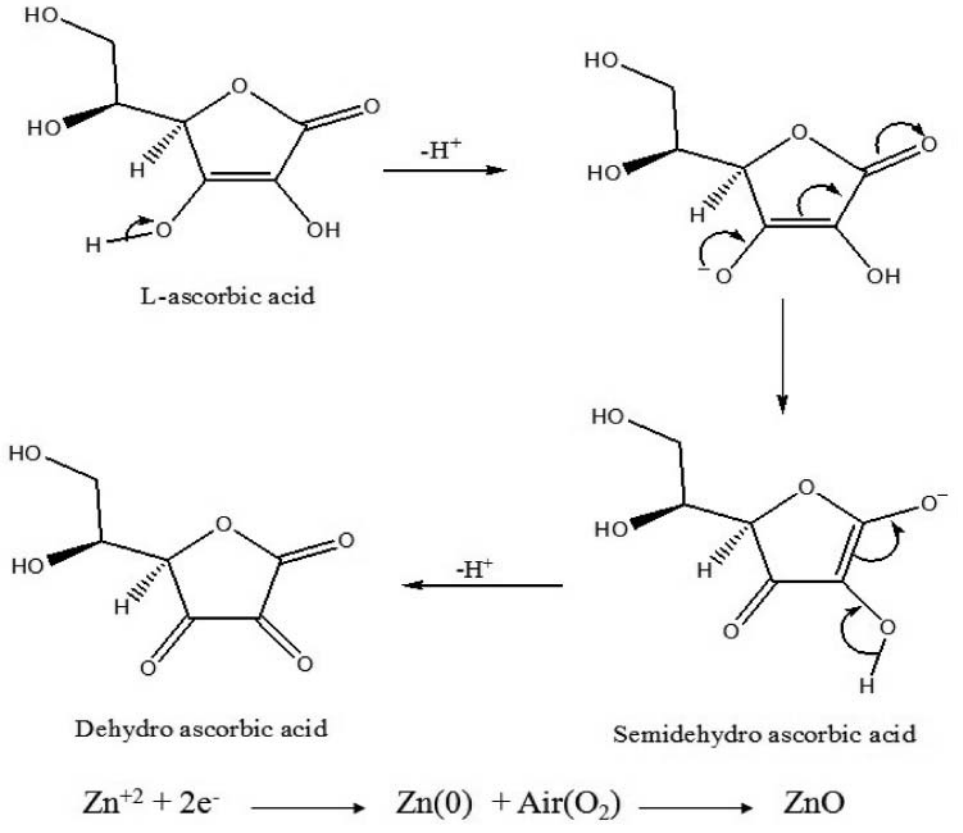

Scheme 1. Reaction of formation of ZnONPs.

2.1.1. Preparation of ZnONPs using tomato extract

Zinc nitrate was used as precursor for the synthesis of ZnONPs. 1:3 ratio of zinc nitrate and tomato extract were mixed and the solution was subjected to heating at 80 °C for 5 min. Same ratio of the solutions were also subjected to microwave irradiation at different power of 180, 360 and 540 W, which produced brown to brownish-black precipitates after 5 min in case of 360 and 540 W. The precipitates were filtered and dried in hot air oven for 4–5 h. The possible mechanism of the formation of ZnONPs from tomato extract was shown in Scheme 1.

2.2. Characterisation ZnONPs

ZnONPs obtained in each case were characterised by dynamic light scattering (DLS; nanotrac wave W3222), UV–visible spectroscopy (UV–vis; Shimadzu 1800), scanning electron microscopy (SEM; JSM-6360 JEOL), X-ray diffraction (XRD; Bruker D8 ADVANCE), atomic force microscopy (AFM; multimode V8) and florescence spectroscopy (Perkin Elmer LS 55).

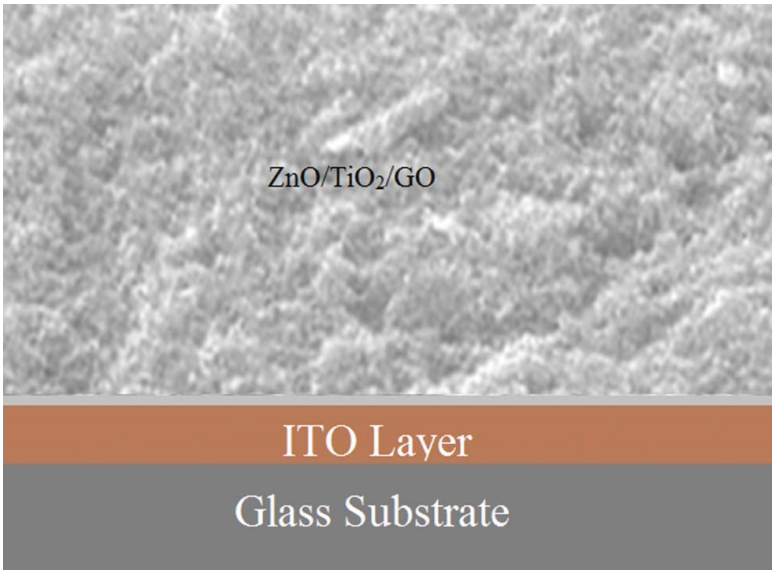

Figure 1. A schematic view of the ZnO/GO/TiO_2 solar cell.

2.3. Preparation of thin films of ZnO nanocomposites

To study the current–voltage performance, different combinations of ZnO nanocomposites were prepared using GO and TiO_2 viz. only ZnO, ZnO/GO (2:1) and ZnO/GO/TiO_2 (2:1:1). The mixtures were sonicated for 30 min followed by stirring at 60 °C for 4 h. The resultant slurry was spread on ITO-coated glass substrate and thin film obtained was dried at 50 °C –60 °C for 1 h in hot air oven. Figure 1 showed a schematic view of the fabricated ZnO/TiO_2/GO-based solar cell.

2.4. Photovoltaic measurements

The photovoltaic measurements of thin films were carried out using a PGSTAT 101 solar simulator with an irradiance of 100 mWcm^{-2}. The current–voltage characteristics of the cell were measured by applying external potential bias to the cell and measuring the generated photocurrent. The monochromator was incremented through the visible spectrum to generate the IPCE (incident photon to current conversion efficiency). Parameters such as short-circuit photocurrent (J_{SC}), open-circuit photovoltage (V_{OC}), fill factor (FF) and efficiency of the solar cell (η) were measured for all the thin films.

3. Results and discussion

3.1. Characterisation of ZnONPs and nanocomposites

The tomato extract was used as reducing as well as stabilising agent for the synthesis of ZnONPs. In order to optimise the reaction conditions and to get good yield of products, the synthesis have been carried out thermally and under microwave irradiation using

different power. No precipitate was observed after heating at 80 °C for 5 min. Microwave irradiation accelerated the synthesis but the yield of the nanoparticles at 180 W after 5 min was very poor. However at 540 W, good yield of ZnONPs was observed after 5 min. The reaction does happen in the absence of microwave heating but it takes almost 4–5 hrs under thermal conditions.

The reaction mechanism in Scheme 1 showed that ZnONPs can be obtained through the reduction of Zn^{+2} using tomato extract, which contains ascorbic acid (32%). Ascorbic acid is a highly water-soluble compound with strong polarity, which acted as both reducing as well as capping agent during the synthesis. As illustrated in Scheme 1, ascorbic acid served as a stable (electron + proton) donor during interactions and was first converted into the radical ion called 'semihydro-ascorbic acid' and then dehydro-ascorbic acid through oxidation. It was suggested that dehydro-ascorbic acid and ascorbic acid together constituted the redox system, which was enough to reduce Zn^{2+} to Zn. Also, the lone pair electrons at the polar groups of ascorbic acid may have occupied two sp orbitals of the zinc ion to form a complex compound. Thus, ascorbic acid was capped with zinc ions and then gave Zn (0) nanoparticles through the reduction of Zn^{2+} inside the nanoscopic templates. In the presence of nanoscopic templates, small zinc nanoparticles were easily formed.

The other explanation may be attributed to the dispersion effect of the oxidation product of ascorbic acid on the zinc nanoparticles after the completion of the reduction reaction. The formation of good yield of ZnONPs at 540 W gave strong evidence for the involvement of ascorbic acid of tomatoes in the rapid biosynthesis and for the stability of metal nanoparticles in the aqueous medium. The synthesis was initially monitored by the colour change (from yellow to dark brown) occurring during the reaction period (Figure 2) and this colour change was obviously due to the excitation of surface plasmon resonance in the metal nanoparticles, indicating the formation of ZnONPs.

The UV–vis spectra of ZnONPs showed the absorption peak at 322 and 334 nm for 360 and 540 W, respectively (Figure 3), which is the characteristic peak range of ZnONPs. From the UV–vis curves, it was further confirmed that at 80 °C and at low microwave power of 180 W, no distinct surface plasmon resonance phenomenon could be observed suggesting that lower microwave power was not sufficient for the formation of ZnONPs within a short time of 5 min. As the power level was increased, surface plasmon peak began to evolve and finally at 540 W, a well-defined and broad peak was observed. Thus, 540 W was required to promote greater amount of nuclei within the time limit of 5 min,

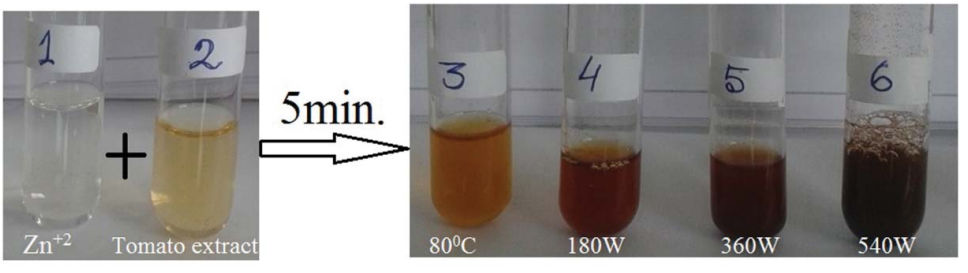

Figure 2. (Colour online) (1) aqueous solution of zinc nitrate; (2) tomato extract; (3–6) colour change under different microwave power.

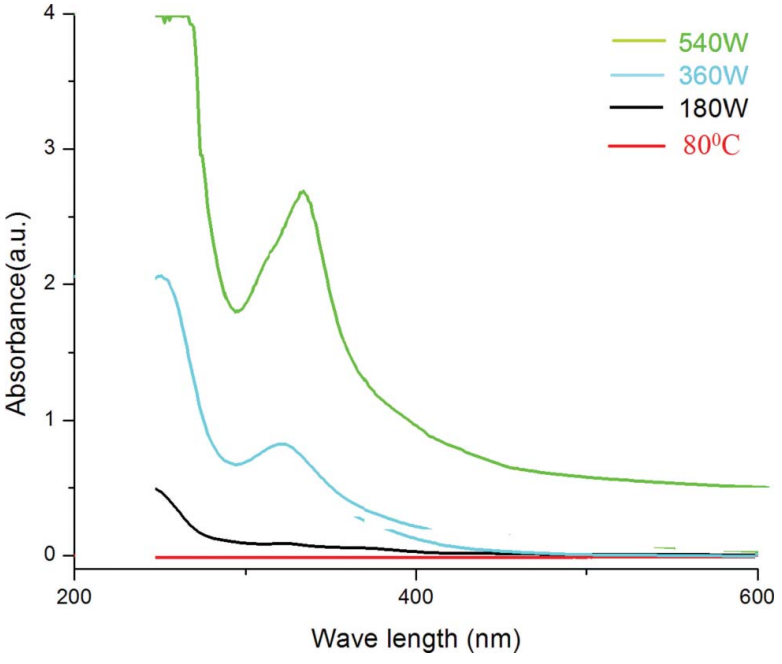

Figure 3. UV−vis spectra of ZnONPs at different microwave power.

which therefore gave greater concentration of nanoparticles in the dispersion. The wave length of the synthesised ZnONPs was found to increase slightly with the increase of power, showing the values of 322 and 334 nm at 360 and 540 W, respectively. The band gap was calculated and interestingly found to be decreased from the values of 3.50 eV at 360 W to 3.38 eV at 540 W.

Figure 4 showed the FTIR of the synthesised ZnONPs at different microwave power. This indicated that the synthesised ZnONPs have good crystallinity and are of high purity. The spectra at 80 °C was not so clear but in all the cases, the peaks at 1381 and 1632 cm^{-1} represented the unreacted ketone group suggesting the presence of flavonones (highly soluble in water) adsorbed on the surface of ZnONPs. This is an important observation which indicated the influence of water soluble organic moieties of tomatoes for their synthesis and surface modification. The FTIR spectra also showed a broad absorption band at 3435 cm^{-1} mainly due to OH groups on the surface of the nanoparticles. All the spectra showed a peak at 530 cm^{-1} which is the characteristic peak of ZnONPs but it was very sharp at 540 W.

The particle size distribution of the ZnONPs formed at different microwave power was carried out at 25 °C using DLS. Figure 5 showed the average particle size distribution of around 20 and 70 nm at 360 and 540 W, respectively. Thus, the average size of the particles which were found to be smaller (20 nm) at low power of 360 W increased upto 70 nm at 540 W after 5 min of irradiation. This indicated that for higher temperature, the reaction was relatively fast and formation as well as growth of the particles was complete. The SEM image of ZnONPs formed at 540 W, clearly indicated their spherical shape and the size between 50 and 90 nm (Figure 6(a)). AFM showed the topographic image of

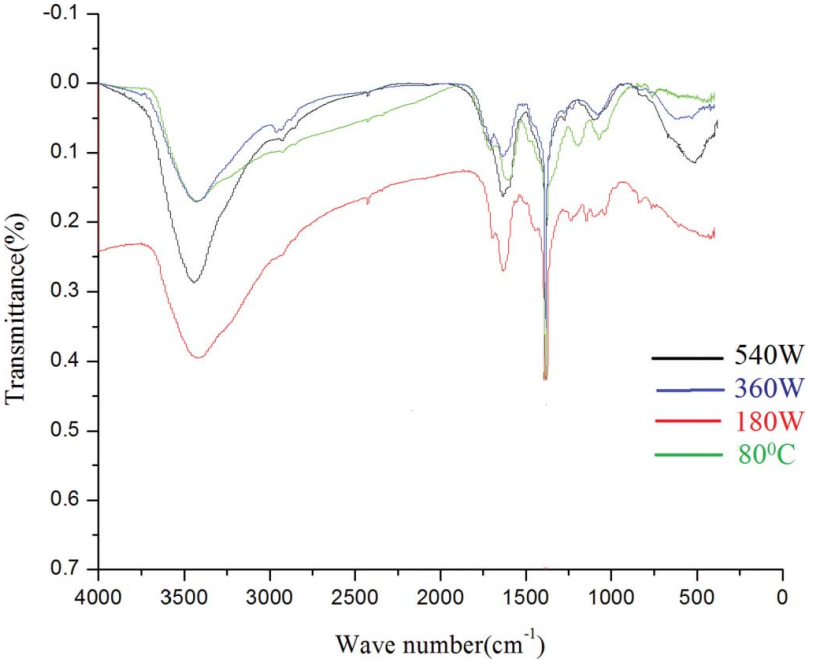

Figure 4. Infra-red spectra of ZnONPs at different microwave power.

well-dispersed ZnONPs at 540 W (Figure 6(b)), which further confirmed the size of the nanoparticles of around 60–70 nm. Figure 6(c) shows that the TEM micrograph of ZnONPs synthesised at 540 W. The TEM micrograph of the ZnONPs confirmed that the particles were almost spherical in shapes with a size range from 40 to 100 nm. Figure 7 showed the XRD pattern of ZnONPs synthesised at 540 W using tomato extract. It showed strong diffraction peaks at 31, 34, 37, 47, 51, 55, 63, 67 and 69 degrees of 2θ which corresponded to (100), (002), (101), (102), (110), (103), (200), (112) and (201) crystal planes.

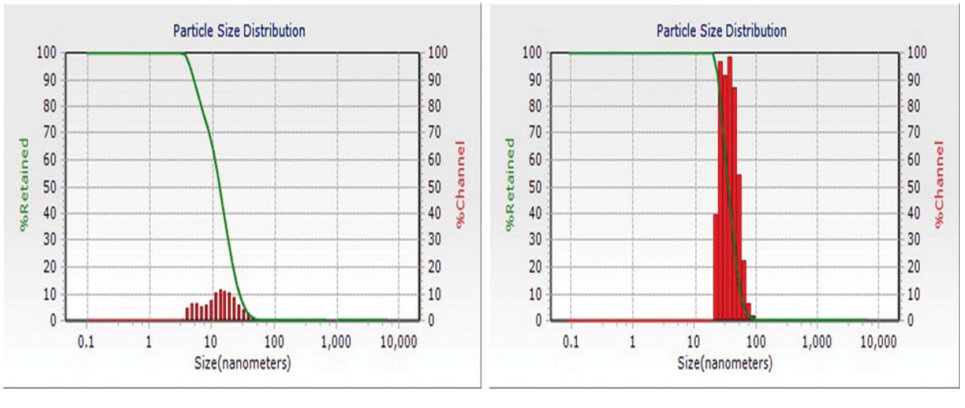

Figure 5. Particle analyser histogram of ZnONPs at 360 and 540 W.

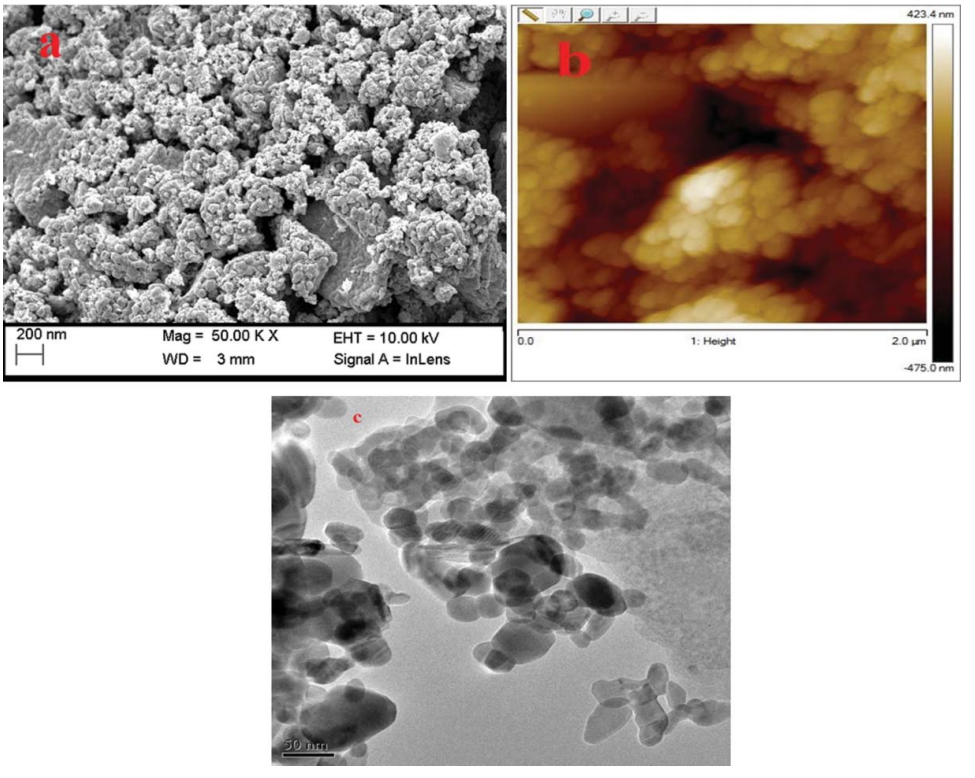

Figure 6. (a) SEM, (b) AFM and (c) TEM image of ZnONPs at 540 W.

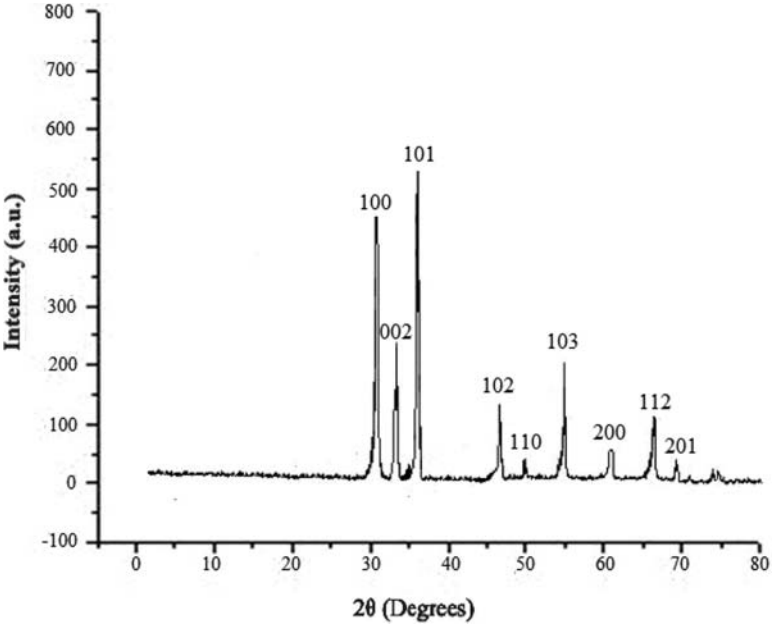

Figure 7. XRD of ZnONPs at 540 W.

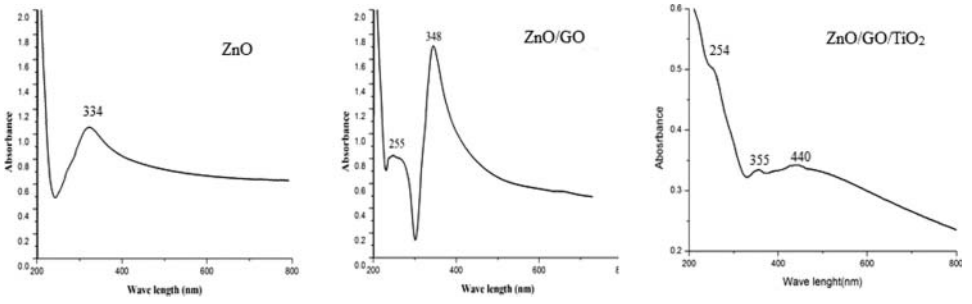

Figure 8. UV−vis spectra of thin films.

The yield of the ZnONPs formed at 540 W was found to be excellent; band gap energy at this power was less as compared to others. Thus, the band gap of ZnONPs was decreased by an increase in temperature and the absorption maximum is also shifted to higher wavelengths [28] and the average particle size (around 70 nm) was also found to be suitable for solar cell applications, so ZnONPs, prepared at 540 W was finally chosen to prepare different nanocomposites. Figure 8 showed the UV−vis spectra of thin films of ZnONPs alone and it's composite with TiO_2 and GO. Since the first curve was the thin film of only ZnONPs, so it showed only one peak at 334 nm. In the second curve of ZnO/GO thin film, two peaks were observed at around 255 and 348 nm indicating the presence of GO and ZnONPs, respectively, in the nanocomposite. In the third curve of ZnO/GO/TiO_2 thin film, three peaks were observed at around 262, 352 and 438 nm confirming the participation of GO and TiO_2 along with ZnONPs.

Figure 9 showed the SEM image of ZnO/GO/TiO_2 nanocomposite, where the size of the particles was around 60−70 nm. It was further confirmed from the AFM image of the nanocomposite given in Figure 10. Figure 11 showed the XRD pattern of ZnO/GO/TiO_2

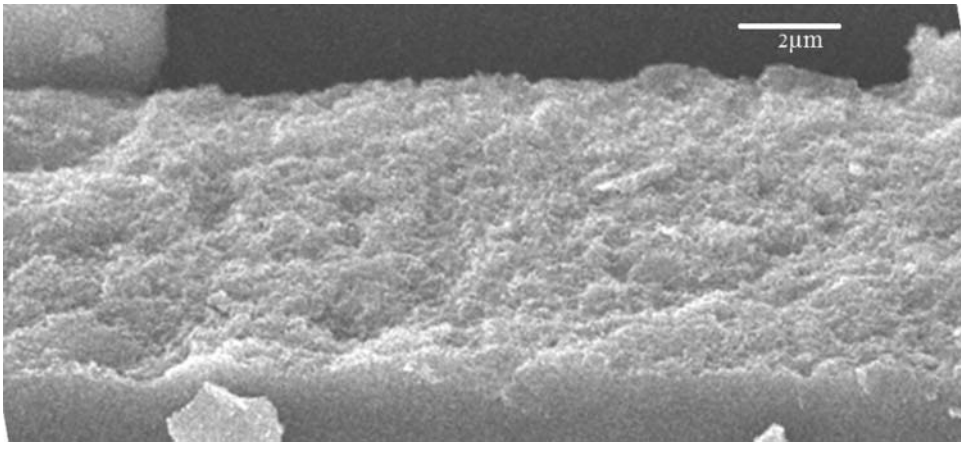

Figure 9. SEM image of thin film of ZnO/GO/TiO_2.

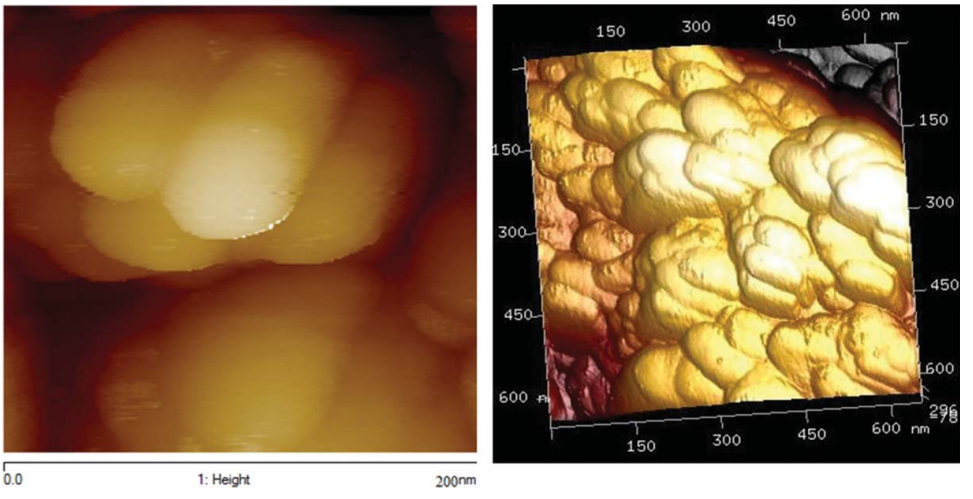

Figure 10. AFM of thin film of ZnO/GO/TiO_2.

nanocomposite. The spectra showed the characteristics peaks at 31, 34, 37, 47, 51, 55, 63, 67 and 69 degrees of 2θ corresponding to (100), (002), (101), (102), (110), (103), (200), (112) and (201) crystal planes of ZnO. The characteristics peaks at 26, 30, 34 and 62 degrees of 2θ corresponded to (101), (004), (200) and (204) crystal planes of TiO_2, whereas the peaks at 10 degrees of 2θ was due to (001) plane of GO.

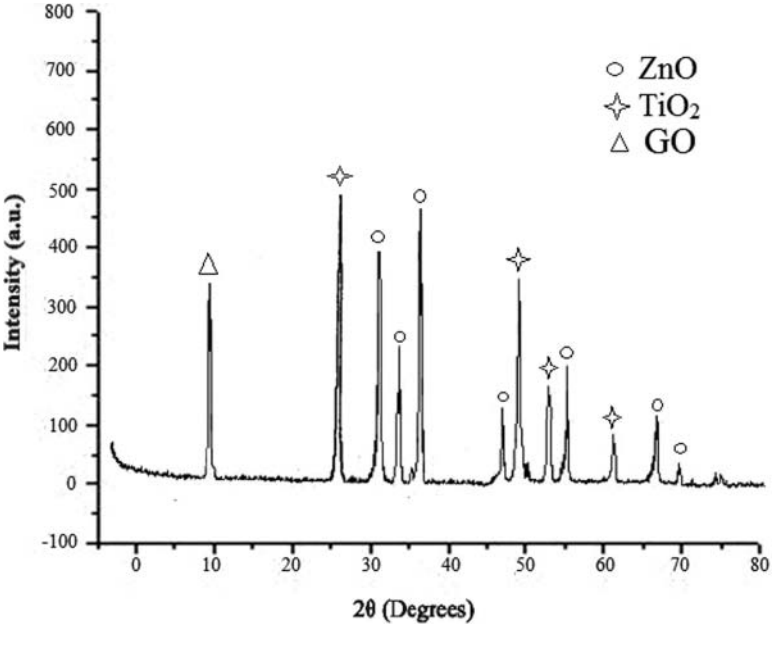

Figure 11. XRD of thin film of ZnO/GO/TiO_2.

3.2. *Photovoltaic performance*

The photovoltaic measurements were carried out with the thin films of ZnO, ZnO/GO and ZnO/GO/TiO_2 nanocomposites using two electrode systems. Xenon lamp was used as a light source and the incident light intensity was maintained at 100 mWcm^{-2}. Figure 12 showed the photocurrent density–voltage measurements ($J-V$ curves) which can be obtained by applying a potential scan, from 0V (short-circuit conditions) to the open-circuit potential, under constant illumination. Under the irradiation of 100 mWcm^{-2}, the measured data for the three nanocomposites were shown in Table 1.

The FF was calculated by [29]

$$\mathrm{FF} = V_{\mathrm{M}} J_{\mathrm{M}} / V_{\mathrm{oc}} J_{\mathrm{sc}},$$

where V_{M} and J_{M} are the photovoltage and photocurrent density for maximum power output, respectively.

Efficiency was calculated by [29]

$$\eta = V_{\mathrm{oc}} J_{\mathrm{sc}} \mathrm{FF} / P_{\mathrm{in}},$$

where P_{in} was the power of incident white light from Xe lamp.

It was observed from the table that V_{oc} values decreased from 0.612 for ZnO to 0.512 for ZnO/GO/TiO_2. FF increased from a value of 0.52 to 0.69 for ZnO/GO/TiO_2. All the three thin films gave good efficiencies but interestingly, the efficiency of the ZnO/GO/TiO_2 nanocomposie showed the maximum value of 6.18%.

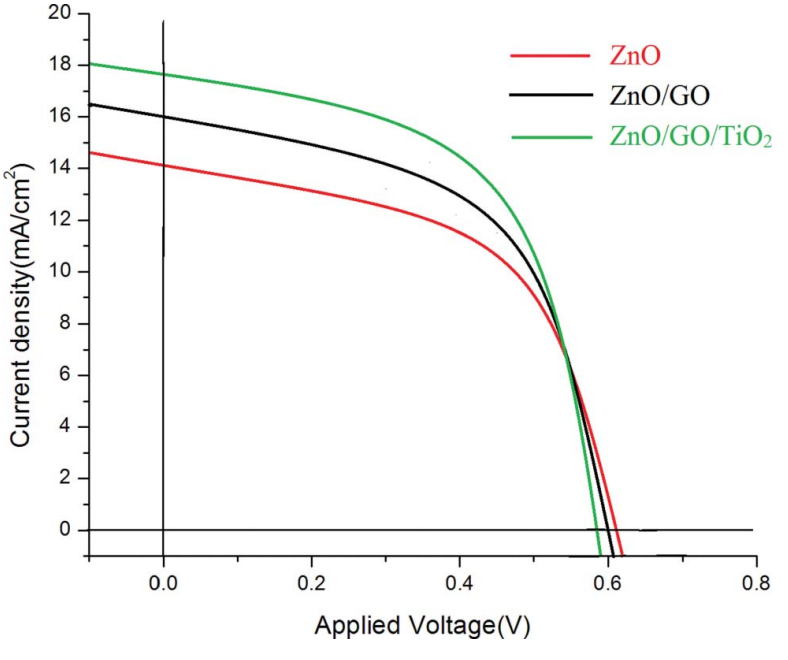

Figure 12. $J-V$ curve of thin films.

Table 1. Current voltage performance of thin films of ZnO, ZnO/GO and ZnO/GO/ TiO_2.

Composite	V_{oc} (V)	J_{sc} (mA cm^{-2})	FF	η (%)
ZnO	0.612	14.4	0.52	4.61
ZnO/GO	0.606	15.8	0.55	5.26
ZnO/GO/ TiO_2	0.512	17.4	0.69	6.18

4. Conclusion

In this work, microwave-assisted green chemistry has been used for the synthesis of ZnONPs. A facile approach has been reported using tomato extract, acting as reducing agent for the synthesis of ZnONPs of well-defined dimensions in bulk amount. This eliminated the need of toxic chemicals for the synthesis of nanoparticles. Besides, excellent reproducibility of these nanoparticles, without the use of any additional capping agent or stabiliser will have a great advantage in comparison with microbial synthesis, avoiding all the tedious and hygienic complications. To optimise the conditions, the synthesis has been done by thermal method as well as under microwave irradiation using different power and the synthesised nanoparticles was successfully used to prepare nanocomposites for photovoltaic application. The current–voltage measurements of the nanocomposites demonstrated enhanced power conversion efficiency of 6.18% in case of ZnO/GO/TiO_2 nanocomposite.

Acknowledgements

The authors express their gratitude to the Director, National Institute of Technology, Agartala for allowing to publish the results. We acknowledge CRF, NIT Agartala and NEHU, Shillong, for the characterisations of nanoparticles.

Disclosure statement

No potential conflict of interest was reported by the authors.

Funding

Financial assistance from CPRI, Bangalore is greatly acknowledged.

References

[1] Nomura K, Ohta H, Ueda K, et al. Thin-film transistor fabricated in single-crystalline transparent oxide semiconductor. Science. 2003;300:1269–1272.
[2] Nakada T, Hirabayashi Y, Tokado T, et al. Novel device structure for Cu(In,Ga)Se2 thin film solar cells using transparent conducting oxide back and front contacts. Sol Energy. 2004;77:739–747.
[3] Lee SY, Shim ES, Kang HS, et al. Fabrication of ZnO thin film diode using laser annealing. Thin Solid Films. 2005;437:31–34.

[4] Könenkamp R, Word RC, Schlegel C. Vertical nanowire light-emitting diode. Appl Phys Lett. 2004;85:6004–6006.
[5] Wang J, Sallet V, Jomard F, et al. Influence of substrate temperature on N-doped ZnO films deposited by RF magnetron sputtering. Thin Solid Films. 2007;515:8785–8788.
[6] Wang ZL. Zinc oxide nanostructures: growth, properties and applications. J Phys Condens Matter. 2004;16:829–858.
[7] Bao D, Gu H, Anxiang K. Anxiang. Sol-gel derived c-axis oriented ZnO thin films. Thin Solid Films. 1998;312:37–39.
[8] Sabbar EH, Saleh MH, Mohammed SS. A fabricated solar cell from ZnO/a-Si/polymers. Int J Adv Sci Technol. 2012;44:89–98.
[9] Bora T, Kyaw HH, Sarkar S, et al. Highly efficient ZnO/Au Schottky barrier dye-sensitized solar cells: Role of gold nanoparticles on the charge-transfer process. Beilstin J Nanotechnol. 2011;2:681–690.
[10] Amornpitoksuk P, Suwanboon S, Sangkanu S, et al. Synthesis, photocatalytic and antibacterial activities of ZnO particles modified by diblock copolymer. Powder Technol. 2011;212:432–438.
[11] Liu J, Qiao SZ, Lu GQ. Magnetic nanocomposites with mesoporous structures: synthesis and applications. Small. 2011;7:425–443.
[12] Grass LRN, Athanassiou EK, Stark WJ. Bottom-up fabrication of metal/metal nanocomposites from nanoparticles of immiscible metals. Chem Mater. 2010;22:155–160.
[13] Tiwari DK, Behari J, Sen P. Time and dose-dependent antimicrobial potential of Ag nanoparticles synthesized by top-down approach. Curr Sci. 2008;95:647–655.
[14] Mohanpuria P, Rana NK, Yadav SK. Biosynthesis of nanoparticles: technological concepts and future applications. J Nanopart Res. 2008;10:507–517.
[15] Honary S, Barabadi H, Gharaei-Fathabad E, et al. Green synthesis of copper oxide nanoparticles using Penicillium aurantiogriseum, Penicillium citrinum and Penicillium waksmanii. Digest J Nanomater Biostruct. 2012;7:999–1005.
[16] Barman G, Maiti S, Laha JK. Bio-fabrication of gold nanoparticles using aqueous extract of red tomato and its use as a colorimetric sensor. Nanoscale Res Lett. 2013;8:181–190.
[17] Capek I. Preparation of metal nanoparticles in water-in-oil (w/o) microemulsions. Adv Colloid Interface Sci. 2004;110:49–74.
[18] Table A, Petit C, Pileni MP. Synthesis of highly monodisperse silver nanoparticles from AOT reverse micelles: A way to 2D and 3D self-organization. Chem Mater. 1997;9:950–959.
[19] Yin B, Ma H, Wang S, et al. Electrochemical synthesis of silver nanoparticles under protection of poly (N-vinylpyrrolidone). J Phys Chem B. 2003;107:8898–8904.
[20] Zhu J, Liu SW, Palchik O, et al. Shape-controlled synthesis of silver nanoparticles by pulse sonoelectrochemical methods. Langmuir. 2000;16:6396–6399.
[21] Sutradhar P, Saha P, Maiti D. Microwave synthesis of copper oxide nanoparticles using tea leaf and coffee powder extracts and its antibacterial activity. J Nanostruct Chem. 2014;4:86–92.
[22] Chandran SP, Chaudhary M, Pasricha R. Synthesis of gold nanotriangles and silver nanoparticlesusing aloe vera plant extract. Biotechnol Prog. 2006;22:577–583.
[23] Sharma N, Kumar J, Thakur S, et al. Antibacterial study of silver doped zinc oxide nanoparticles against Staphylococcus aureus and Bacillus subtilis. Drug Invention Today. 2013; 5:50–54.
[24] Sangeetha G, Rajeshwari S, Venckatesh R. Green synthesis of zinc oxide nanoparticles by aloe barbadensis miller leaf extract: Structure and optical properties. Mater Res Bull. 2011;46:2560.
[25] Jayaseelan C, Rahuman AA, Kirthi AV, et al. Novel microbial route to synthesize ZnO nanoparticles using Aeromonas hydrophila and their activity against pathogenic bacteria and fungi. Spectrochim Act A Mol Biomol Spectrosc. 2012;90:78–84.
[26] Jain N, Bhargava A, Tarafdar JC, et al. A biomimetic approach towards synthesis of zinc oxide nanoparticles. J Appl Microbiol Biotechnol. 2013;97:859–869.

[27] Shahriary L, Athawale AA. All rights reserved graphene oxide synthesized by using modified hummers approach. Int J Renew Energy Environ Eng. 2014;02:58–63.
[28] Surabhi SK, Putcha V, Vanka RR, et al. Synthesis, characterization and optical properties of zinc oxide nanoparticles. Int Nano Lett. 2013;3:30–35.
[29] Waltera MG, Rudineb AB, Wamser CC. Porphyrins and phthalocyanines in solar photovoltaic cells. J Porphyrin Phthalocyanines. 2010;14:759–792.